

# SSSAJ

Soil Science Society of America Journal





# Suggestions for Contributors to the *Soil Science Society of America Journal*

## General Requirements

Contributions to the *Soil Science Society of America Journal* (SSSAJ) may be (i) papers and notes on original research; and (ii) "Comments and Letters to the Editor" containing (a) critical comments on papers published in one of the Society outlets or elsewhere, (b) editorial comments by Society officers, or (c) personal comments on matters having to do with soil science. Notes are not to exceed two printed pages. Letters to the Editor are limited to one printed page. Contributions need not have been presented at annual meetings. Original research findings are interpreted to mean the outcome of scholarly inquiry, investigations, modeling, or experimentation having as an objective the revision of existing concepts, the development of new concepts, or the development of new or improved techniques in some phase of soil science. Authors are encouraged to test modeling results with measurements or published data. Short critical reviews or essays on timely subjects, upon invitation by the Editorial Board, may be published on a limited basis. The SSSAJ also invites submissions for cover illustrations from authors of manuscripts accepted for publication. Refer to SSSA Publication Policy [Soil Sci. Soc. Am. J. 65(1): v-vii, 2001] and to the *Publications Handbook and Style Manual* (ASA-CSSA-SSSA, 1998) for additional information.

The SSSAJ uses a double blind review format. Authors are anonymous to reviewers and reviewers are anonymous to authors. A detachable title page includes title, author(s), author-paper documentation, and acknowledgments. The manuscript title but not the authors are repeated on the abstract page. The *Publications Handbook and Style Manual* (1998) (<http://www.asa-cssa-sssa.org/style98/>) is the official guide for preparation and editing of papers. Copies are available from ASA Headquarters, 677 S. Segoe Rd., Madison, WI 53711 (books@agronomy.org).

## Submitting Manuscripts

Manuscripts can be submitted to the SSSAJ Editor as PDF files. Detailed instructions for creating and uploading PDF files can be found at <http://www.manuscripttracker.com/ssaj/> along with instructions related to logging on to the SSSAJ Manuscript Tracker system.

Alternatively, authors may send four legible double-spaced copies of each manuscript on 21.6- by 27.9-cm paper. The lines of type must be numbered on each page, and at least 2.5-cm margins left on top, bottom, and sides. Pages should be numbered consecutively. Type legends for figures (double spaced) on one or more sheets and place at the end of the manuscript.

A cover letter should accompany each submission. Send the copies to:

Dr. Richard L. Mulvaney, Editor  
Soil Science Society of America Journal  
University of Illinois  
1102 South Goodwin Avenue  
Urbana, IL 61801  
e-mail: mulvaney@uiuc.edu

**Potential Reviewers.** Authors who submit manuscripts as hard copies or through the SSSAJ Manuscript Tracker system will be encouraged to provide a list of potential reviewers. Those who do not use Manuscript Tracker are encouraged to include a cover letter along with their submission that suggests potential reviewers. Reviewers must not have a conflict of interest involving the authors or paper and the editorial board has the right not to use any reviewers suggested by authors.

## Creating the Manuscript Files

Although manuscript review is done electronically or with printed copies, accepted manuscripts are edited as word processing files. Therefore, authors should keep in mind the following when preparing manuscript files.

All accepted manuscript files will ultimately be converted to Microsoft Word format for on-screen editing. Therefore, files that are originally composed in or converted to Microsoft Word are strongly preferred. Other formats are also acceptable, but authors should be aware that errors are occasionally introduced during the conversion process. Furthermore, authors should avoid using word processing features such as automated bulleting and numbering, footnoting, head and subhead formatting, internal linking, or styles. Avoid using more

than one font and font size. Limited use of italics, bold, superscripts, and subscripts is acceptable. The file should be double spaced and line numbered, with at least 2.5-cm margins. Rich-text format (.rtf extension) and TeX files are not acceptable.

**Title Page.** The title page should include:

1. A short title not exceeding 12 words. The title should accurately identify and describe the manuscript content.
2. An author-paper documentation. Include author name(s), sponsoring organization(s), and complete address(es). Identify the corresponding author with an asterisk (\*). Professional titles are not listed. Other information such as grant funding, may be included here or placed in an acknowledgment, also on the title page. To ensure an unbiased review, the title page will be removed during the review process. The title, but not the byline, should therefore be repeated on the page that contains the abstract.
3. An abbreviations list. Include abbreviations that are used repeatedly throughout the manuscript. Do not list SI units, chemical element symbols, or variables from equations.
4. The corresponding author's phone and fax numbers and e-mail address.

**Abstract.** An informative, self-explanatory abstract, not exceeding 250 words (150 words for notes), must be supplied on a separate page. It should specifically tell why and how the study was made, what the results were, and why they were important. Use quantitative terms. The title should be repeated on top of the abstract page without author identification.

**Tables.** Each table must be on a separate page and numbered consecutively. Do not duplicate matter that is presented in charts or graphs. Use the following symbols for footnotes in the order shown: †, ‡, §, ¶, #, ††, ‡‡, . . . etc.

The symbols \*, \*\*, and \*\*\* are always used to show statistical significance at 0.05, 0.01, and 0.001 levels, respectively, and are not used for other footnotes. Spell out abbreviations on first mention in tables, even if the abbreviation is defined in the text (i.e., a reader should be able to understand the table contents without referring back to the text).

**Figures.** Do not use figures that duplicate matter in tables. Photographs for halftone reproduction should be glossy prints with good dark and light contrast. When creating figures, use font sizes and line weights that will reproduce clearly and accurately when figures are sized to the appropriate column width. The minimum line weight is 1/2 point (thinner lines will not reproduce well). Screening and/or shaded patterns often do not reproduce well; whenever possible, use black lines on a white background in place of shaded patterns.

Authors can reduce manuscript length and, therefore, production charges, by supplying photographs and drawings that can be reduced to a one-column width (8.5 cm or 20 picas). Lettering or numbers in the printed figure should not be smaller than the type size in the body of an article as printed in the journal (8-point type) or larger than the size of the main subheads (12-point type). The minimum type size is 6-point type. As an example, a 17-cm-wide figure should have 16-point type, so that when the figure is reduced to a single column, the type is reduced to 8-point type.

Label each figure with the title of the article and the figure number. Type captions in the word processing file following the references. As with tables, spell out abbreviations on first mention in figure captions, even if they have already been defined in the text.

**References.** When preparing the reference list, keep in mind the following:

1. Do not number the references listed.
2. Arrange the list alphabetically by the names of the first authors and then by the second and third authors.
3. Single-authored articles should precede multiple-authored articles for which the individual is senior author.
4. Two or more articles by the same author(s) are listed chronologically; two or more in the same year are indicated by the letters a, b, c, etc.
5. All published works referred to in the text must be listed in the reference list and vice versa.
6. Only literature that is available through libraries can be cited. The reference list can include theses, dissertations, and abstracts.
7. Material not available through libraries, such as personal com-

munications or privileged data, should be cited in the text in parenthetical form.

8. Chapter references from books must include, in order, authors, year, chapter or article title, page range, editor(s), book title, publisher, and city.
9. Symposium proceedings should include editor, date and place of symposium, publisher, and page numbers.

### Style Guidelines

All soils discussed in publications should be identified according to the U.S. soil taxonomic system the first time each soil is mentioned. The Latin binomial or trinomial and authority must be shown for all plants, insects, pathogens, and animals when first mentioned. Both the accepted common name and the chemical name of pesticides must be provided. SI units must be used in all manuscripts. Corresponding metric or English units may be added in parentheses at the discretion of the author. If a commercially available product is mentioned, the name and location of the manufacturer should be included in parentheses after first mention.

### Official Sources

1. Spelling: Webster's *New Collegiate Dictionary*
2. Amendments to the U.S. system of soil taxonomy (Soil Survey Staff, 1975) have been issued in the *National Soil Survey Handbook* (NRCS, 1982–1996) and in *Keys to Soil Taxonomy* (Soil Survey Staff, 1996). Updated versions of these and other resources are available at <http://www.statlab.iastate.edu/soils/index.html>
3. Scientific names of plants: *A Checklist of Names for 3000 Vascular Plants of Economic Importance* (USDA Agric. Handb. 505, see also the USDA Germplasm Resources Information Network database, <http://www.ars-grin.gov/npgs/searchgrin.html>)
4. Chemical names of pesticides: *Farm Chemicals Handbook* (Meister Publishing, revised yearly)
5. Soil series names: *Soil Series of the United States, Including Puerto Rico and the U.S. Virgin Islands* (USDA-SCS Misc. Publ. 1483, <http://www.statlab.iastate.edu:80/soils/osd>)
6. Fungal nomenclature: *Fungi on Plants and Plant Products in the United States* (APS Press)
7. Journal abbreviations: *Chemical Abstracts Service Source Index* (American Chemical Society, revised yearly)
8. *The Glossary of Soil Science Terms* is available both in hard copy (SSSA, 1997) and on the SSSA Web page ([www.soils.org/ssagloss/](http://www.soils.org/ssagloss/)). It contains definitions of more than 1800 terms, a procedural guide for tillage terminology, an outline of the U.S. soil classification system, and the designations for soil horizons and layers.

### Manuscript Revisions

Authors have three months to make revisions and return their manuscripts following reviewer and associate editor comments. If not re-

turned within three months, the manuscript will be released; it must then be resubmitted as a new paper.

### Length of Manuscript and Page Charges

Membership in the Society is not a requirement for publication in the SSSAJ; however, nonmembers will be charged an additional amount for the first six published pages of a manuscript. To qualify for member rates, at least one author must be an active, emeritus, graduate student, or undergraduate student member of SSSA, CSSA, or ASA on the date the manuscript is accepted for publication. Volunteered papers will be assessed a charge of \$25 per page for nonmembers for each printed page from page one through page six; a charge of \$190 per page (\$95 per half page) will be assessed all papers for additional pages. No charges will be assessed against invited review papers or comments and letters to the editor. The Society absorbs the cost of reproducing illustrations up to \$15 for each paper.

In general, four manuscript pages will equal one printed page. For space economy, Materials and Methods, long Literature Reviews, theory, soil or site descriptions, etc., footnotes, tables, figure captions, and references are set in small type. Each table and figure will usually take 1/4 of a printed page. For tabular matter, 9 lines of typewritten matter equal 1 column-inch of type. Allow also for rules and spacing. Tables with more than 35 units (including space between words) in a horizontal line can rarely be set 1 page-column wide. The depth of a printed figure will be in the same proportion to the width (1 column = 8.5 cm; 2 column = 17.2 cm) as that of the corresponding dimensions in the original drawing.

Authors can publish color photos, figures, or maps at their own expense. Please call the Managing Editor (608-273-8095) for price information.

### Accepted Manuscripts

Following hard copy submission and review, both a printed copy and word processing file of the final accepted manuscript are required. The printed copy and word processing file must match exactly in all parts of the manuscript. Printed copies and files for tables and figures must also be included. The files for text, tables, and figures should be separate.

Send the printed copy and a disk with the manuscript files to:

Nicholas Rhodehamel, Managing Editor, SSSAJ  
American Society of Agronomy  
677 South Segoe Road  
Madison, WI, USA 53711

Alternatively, if the paper was submitted for review through the SSSAJ Manuscript Tracker system, the final accepted version can be uploaded as a Word file at <http://www.manuscripttracker.com/ssaj/finaldocs.htm>. A printed copy that exactly matches the word processing file must still be sent to the address listed above.

Questions? Send your questions to Nicholas Rhodehamel, Managing Editor, SSSAJ ([nrhodehamel@agronomy.org](mailto:nrhodehamel@agronomy.org)).

July 2002

**Division S-1—Soil Physics**

- 1–11 Modeling Ammonia Volatilization from Surface-Applied Swine Effluent. *J. Wu, D.L. Nofziger, J.G. Warren, and J.A. Hattey*
- 12–19 Pore-Space Dynamics in a Soil Aggregate Bed under a Static External Load. *Teamrat A. Ghezzehei and Dani Or*
- 20–31 Oxygen Transport to Plant Roots: Modeling for Physical Understanding of Soil Aeration. *F.J. Cook and J.H. Knight*
- 32–40 Air Permeability in Undisturbed Volcanic Ash Soils: Predictive Model Test and Soil Structure Fingerprint. *Per Moldrup, Seiko Yoshikawa, Torben Olesen, Toshiko Komatsu, and Dennis E. Rolston*
- 41–51 Gas Diffusivity in Undisturbed Volcanic Ash Soils: Test of Soil-Water-Characteristic-Based Prediction Models. *Per Moldrup, Seiko Yoshikawa, Torben Olesen, Toshiko Komatsu, and Dennis E. Rolston*
- 52–61 Time Domain Reflectometry Field Calibration in the Little Washita River Experimental Watershed. *Gary C. Heathman, Patrick J. Starks, and Michael A. Brown*
- 62–70 Considerations for Improving the Accuracy of Permittivity Measurement using Time Domain Reflectometry: Air-Water Calibration, Effects of Cable Length. *D.A. Robinson, M. Schuan, S.B. Jones, S.P. Friedman, and C.M.K. Gardner*
- 71–76 Evaluation of a Model for Irrigation Management Under Saline Conditions: I. Effects on Plant Growth. *G.L. Feng, A. Meiri, and J. Letey*
- 77–80 Evaluation of a Model for Irrigation Management Under Saline Conditions: II. Salt Distribution and Rooting Pattern Effects. *G.L. Feng, A. Meiri, and J. Letey*
- 81–91 Robust estimation of the generalized solute transfer function parameters. *M. Javaux and M. Vanclooster*
- 92–99 An Instantaneous-Profile Laser Scanner to Measure Soil Surface Microtopography. *Frédéric Darboux and Chi-hua Huang*
- 100–106 An Automated Vacuum Extraction Control System for Soil Water Percolation Samplers. *R.D. Lentz and D.C. Kincaid*

**Division S-1—Notes**

- 107–111 Rapid Water Flow Instrumentation. *Wallace Troyer and J. Skopp*

**Division S-2—Soil Chemistry**

- 112–121 Organic Ligand and pH Effects on Isotopically Exchangeable Cadmium in Polluted Soils. *Richard N. Collins, Graham Merrington, Mike J. McLaughlin, and Jean-Louis Morel*
- 122–131 Sorption and Desorption of Pesticides by Clay Minerals and Humic Acid-Clay Complexes. *Hui Li, Guangyao Sheng, Brian J. Teppen, Cliff T. Johnston, and Stephen A. Boyd*

**Division S-3—Soil Biology & Biochemistry**

- 132–138 Bermudagrass Management in the Southern Piedmont USA. III. Particulate and Biologically Active Soil Carbon. *A.J. Franzluebbers, and J.A. Stuedemann*
- 139–145 Myrosinase Activity in Soil. *Ahmad I. Al-Turki and Warren A. Dick*
- 146–155 Soil Aggregation and Carbon and Nitrogen Pools under Rhizoma Peanut and Perennial Weeds. *U.M. Sainju, T.H. Terrill, S. Gelaye, and B.P. Singh*
- 156–165 Linking Soil Microbial Activity to Water- and Air-Phase Contents and Diffusivities. *Per Schjønning, Ingrid K. Thomsen, Per Moldrup, and Bent T. Christensen*
- 166–180 Non-Flow-Through Steady-State Chambers for Measuring Soil Respiration: Numerical Evaluation of Their Performance. *G.L. Hutchinson and P. Rochette*

**Division S-4—Soil Fertility & Plant Nutrition**

- 181–189 The Role of Particulate Organic Matter in Phosphorus Cycling. *A.M. Salas, E.T. Elliott, D.G. Westfall, C.V. Cole, and J. Six*

**Division S-5—Pedology**

- 190–197 Drainage Network Analysis for Regional Partitions of Alluvial Paddy-Field Soils. *T. Ishida, S. Itagaki, Y. Sasaki, and H. Ando*

*Continued on page ii*



**This issue's cover:** Strongly developed spodosol (Typic Placorthod) in Nörlund Plantation, Western Denmark (56° 05' N lat., 9° 10' E long.), developed on fine eolian sand (cover sand). Two horizons in the profile are particular C rich; the thick humus rich A horizon and the spodic Bh horizon. Spodosols are in general the most C rich soil type in Denmark, and of strong significance in the estimation of total C pools of terrestrial ecosystems. At present the vegetation is spruce, but formerly the location had a long history of extensively managed Calluna heath. For details see "Carbon and Nitrogen in Danish Forest Soils—Contents and Distribution Determined by Soil Order" p. 335–343. (Photographer: Henrik Vejre, 1997).



- 198–207 Genesis of Tephra-derived Soils from the Roccamonfina Volcano, South Central Italy. *A. Vacca, P. Adamo, M. Pigna, and P. Violante*
- 208–214 Soil Survey Mapping Unit Accuracy in Forested Field Plots in Northern Pennsylvania. *P.J. Drohan, E.J. Ciolkosz, and G.W. Petersen*
- 215–224 Using Soil Phosphorus Profile Data to Assess Phosphorus Leaching Potential in Manured Soils. *Peter J.A. Kleinman, Brian A. Needelman, Andrew N. Sharpley, and Richard W. McDowell*
- 225–234 Hillslope Soils and Organic Matter Dynamics within a Native American Agroecosystem on the Colorado Plateau. *J.B. Norton, J.A. Sandor, and C.S. White*

#### **Division S-6—Soil & Water Management & Conservation**

- 235–240 A Single Irrigation to Improve Early Maturing Soybean Yield and Quality. *Daniel W. Sweeney, James H. Long, and M.B. Kirkham*
- 241–250 Roughness Measurements of Soil Surfaces by Acoustic Backscatter. *Michael L. Oelze, James M. Sabatier, and Richard Raspet*
- 251–257 A Unified Framework For Water Erosion And Deposition Equations. *B. Yu*
- 258–267 Soil Carbon Maps: Enhancing Spatial Estimates with Simple Terrain Attributes at Multiple Scales. *T.G. Mueller and F.J. Pierce*
- 268–278 Modeling Slope Stability in Honduras: Parameter Sensitivity and Scale of Aggregation. *Benjamin F. Zaitchik, Harold M. van Es, and Patrick J. Sullivan*
- 279–288 Using Rare-Earth Oxide Tracers for Studying Soil Erosion Dynamics. *X.C. Zhang, M.A. Nearing, V.O. Polyakov, and J.M. Friedrich*
- 289–299 The Spectral Reflectance Properties of Soil Structural Crusts in the 1.2- to 2.5- $\mu\text{m}$  Spectral Region. *E. Ben-Dor, N. Goldshleger, Y. Benyamini, M. Agassi, and D.G. Blumberg*

#### **Division S-7—Forest & Range Soils**

- 300–308 Nitrogen Accumulation by Conifer Seedlings and Competitor Species From  $^{15}\text{N}$ -labeled Controlled-Release Fertilizer. *Ryan D. Hangs, J. Diane Knight, and Ken C.J. Van Rees*
- 309–317 Nitrogen Retranslocation Response of Young *Picea mariana* to Nitrogen-15 Supply. *K.F. Salifu and V.R. Timmer*
- 318–326 Sampling-Induced Increases in Net Nitrification in the Brush Brook (Vermont) Watershed. *Donald S. Ross and Heidi C. Hales*
- 327–334 A Calibration System for Soil Carbon Dioxide-Efflux Measurement Chambers: Description and Application. *Britta Widén and Anders Lindroth*
- 335–343 Carbon and Nitrogen in Danish Forest Soils—Contents and Distribution Determined by Soil Order. *Henrik Vejre, Ingeborg Callesen, Lars Vesterdal, and Karsten Raulund-Rasmussen*

#### **Division S-8—Nutrient Management & Soil & Plant Analysis**

- 344–350 Changes in Bicarbonate-extractable Inorganic and Organic Phosphorus by Drying Pasture Soils. *Benjamin L. Turner and Philip M. Haygarth*
- 351–364 Yield Models Implied by Traditional Fertilizer Recommendations and a Framework for Including Nontraditional Information. *Terry L. Kastens, John P. Schmidt, and Kevin C. Dhuyvetter*

#### **Division S-10—Wetland Soils**

- 365–372 Hillslope Hydrology and Soil Morphology for a Wetland Basin in South-Central Minnesota. *Ron J. Reuter and Jay C. Bell*

#### **Other Items**

- 373 Errata

## **Important Note to Authors**

Recently, the SSSAJ production editing staff has changed systems for preparing accepted manuscripts for typesetting.

The new, more efficient system requires Microsoft Word documents rather than Corel WordPerfect. We strongly encourage you to compose manuscript files in Word.

In addition, the new system can use Word tables. Fewer errors are induced when tables are set from electronic files than, as was formerly done, from hard copy.

Figures are still prepared almost entirely from hard copy. You may compose figures in any software you desire; submit these files but also send hard copies.

For more information, see the updated *Suggestions to Contributors*, this issue of SSSAJ and <http://soil.scijournals.org/misc/ifora.shtml>.

# SOIL SCIENCE SOCIETY OF AMERICA JOURNAL

VOL. 67

JANUARY-FEBRUARY 2003

No. 1

## DIVISION S-1—SOIL PHYSICS

### Modeling Ammonia Volatilization from Surface-Applied Swine Effluent

J. Wu, D. L. Nofziger,\* J. G. Warren, and J. A. Hattey

#### ABSTRACT

Ammonia volatilization is an important issue in agricultural production and environmental protection. Experimental methods and numerical models exist to estimate the rate and amount of ammonia volatilization from commercial fertilizers and animal manures applied to a field. The existing models imposed assumptions on water movement in a soil profile that were judged to be inadequate for surface-applied swine (*Sus Domesticus*) effluent. In this research, a computer model was developed to estimate short-term ammonia volatilization from swine effluent applied to a field by flood or sprinkler irrigation. The model simulates simultaneous water flow, heat flow, and the transport and transformation of ammoniacal N in a soil profile using the finite difference method. Submodels were developed to evaluate concentrations of ammoniacal N in the infiltration pond of a flood irrigation event and in the droplets of sprinkler irrigation. The governing equations for the water flow, heat flow, and chemical transport modules and the irrigation submodules were derived from mass balance and energy balance employing constitutive laws established empirically. The model was tested against data from field experiments using parameters obtained from independent sources. The simulation results were in excellent agreement with experimental data in three out of six experiments. In the other three experiments, the predicted cumulative volatilization exceeded the measured amount by 5 to 30 kg ha<sup>-1</sup> at the end of 1 wk. The differences were primarily in the first sampling period after the application. The simulated cumulative volatilization was most sensitive to temperature, pH of the soil system, and pH of the effluent applied.

AMMONIA VOLATILIZATION from applied N fertilizer and animal manure significantly reduces the amount of ammoniacal N available for crop use. In calcareous soils, over 50% of ammoniacal N from ammonium nitrate (NH<sub>4</sub>NO<sub>3</sub>) incorporated into the topsoils may be lost to ammonia volatilization (Fenn and Escarzag, 1977). Ammonia volatilization is also one of the largest sources of atmospheric ammonia that contributes to soil

acidification and water eutrophication (Asman and van Jarrsveld, 1992; European Centre for Ecotoxicology and Toxicology of Chemicals [E.C.E.T.O.C.], 1994; Sutton et al., 1995). Therefore, enormous effort has been made to quantify ammonia volatilization from the soil surface. In the 1970s and 1980s, laboratory and field experiments were conducted to measure ammonia volatilization from urea incorporated in a soil profile (Fenn and Escarzag, 1977; Khengre and Savant, 1977; McInnes et al., 1985; Reynolds et al., 1985). In the 1990s the integrated horizontal flux method and micrometeorological methods were used to measure ammonia volatilization from slurry and swine effluent applied to land surface (Genermont and Cellier, 1997; Schjoerring et al., 1992; Zupancic et al., 1999). Mathematical models were developed to extend experimental results to different climate-soil management conditions (Genermont and Cellier, 1997; Rachhpal-Singh and Nye, 1986; Kirk and Nye, 1991). Genermont and Cellier's model was developed for estimating ammonia volatilization from surface-applied slurry while Rachhpal-Singh and Nye's and Kirk and Nye's models were for estimating ammonia volatilization from urea incorporated in a soil profile. In the model developed by Genermont and Cellier (1997), Darcy's law was employed to evaluate the flux density of vertical water flow. But no transient flow conditions were considered in the model. Kirk and Nye (1991) expanded Rachhpal-Singh and Nye's (1986) model to account for the effects of transient-state water evaporation, but the model cannot simulate water flow during infiltration. Since none of the above-mentioned models could simulate the infiltration process at the soil surface, they were considered inadequate for simulating transport and transformation of ammoniacal N in a soil profile under swine-effluent irrigation.

The main objective of this research was to develop a mechanistic model to predict short-term (such as a week) ammonia volatilization from swine effluent applied to

Department of Plant and Soil Sciences, Oklahoma State University, Stillwater, OK 74078. This research was supported in part by funds from the Oklahoma Agricultural Experiment Station. Received 26 June 2001. \*Corresponding author (dln@okstate.edu).

Published in Soil Sci. Soc. Am. J. 67:1–11 (2003).

**Abbreviations:** E.C.E.T.O.C., European Centre for Ecotoxicology and Toxicology of Chemicals; IHF, integrated horizontal flux.



a field during and after a flood or sprinkler irrigation event. The case of flood irrigation was included to simulate field experiments. The main body of the model developed in this research simulates simultaneous water flow, heat flow, and the transport and transformation of ammoniacal N in a soil profile using finite difference methods. Submodels were also developed to estimate the concentrations of ammoniacal N in the infiltration pond of a flood irrigation event or the droplets of a sprinkler irrigation event.

### General Description of the Model

The mechanistic ammonia volatilization model consists of modules simulating water infiltration and ammonia volatilization during an irrigation event, water evaporation, and ammonia volatilization from the soil surface after an irrigation event, and transport and transformation of ammoniacal N in a soil profile during and after an irrigation event. The ammonia volatilization model incorporates the effect of the major factors illuminated by previous investigations. These include soil and effluent pH, soil and air temperature, wind speed, application rate of the source of ammoniacal N, soil wetness and soil hydraulic properties (Ismail et al., 1991). The transport-and-transformation module is the main body of the model. It is made up of three submodules simulating water flow, heat flow, and the transport and transformation of ammoniacal N in a soil profile. The water flow and heat flow modules were included to provide information on soil wetness and soil temperature, which were needed for the computation of the parameters in the transport-and-transformation module. The transport-and-transformation module produces concentrations of ammoniacal N at different depths in a soil profile. The rate of ammonia volatilization from soil surface was determined from the concentration of ammoniacal N at the soil surface. The governing equations of all the modules were derived from mass and energy balances. Constitutive relationships such as Darcy's law, Fourier's law, and Fick's law were employed to specify the fluxes of water, heat, and ammoniacal N. Henry's law, the equilibrium constant of the  $\text{NH}_4^+(\text{aq}) \leftrightarrow \text{NH}_3(\text{aq})$  reaction, and linear adsorption-desorption isotherms were used to quantify the transformation among the component ammoniacal N species in a soil system.

The governing equations for water flow and heat flow are well established in the literature (Hillel, 1998; Scott, 2000). The focus of this research is the transport and transformation of ammoniacal N in a soil system. Because of the complexity of the processes involved, the following simplifications were introduced in the derivation of the governing equation for the transport-and-transformation model: (i) soil pH is not affected by the current application of swine effluent; (ii) the transformation reactions among the component species of ammoniacal N reach equilibrium instantaneously; (iii) contribution of ammoniacal N from mineralization of soil organic matter and loss of ammoniacal N through immobilization and nitrification are insignificant compared with volatilization loss for the small time of interest in

this research; (iv) adsorption-desorption reactions of ammoniacal N species in soil follow linear equilibrium isotherms; (v) convective movement of soil air is insignificant and transport of gas-phase ammonia in soil is controlled by diffusion; (vi) transport of liquid-phase ammoniacal N is controlled by the convection-dispersion process.

A submodel for ponded infiltration was developed to estimate ammoniacal N concentration in the ponding layer of a flood-irrigation event. The concentration is needed to specify the upper boundary condition of the transport-and-transformation model during a flood irrigation event. Concentration of ammoniacal N in the ponding layer is also needed for evaluating ammonia volatilization rate during a flood-irrigation event. Equations in the ponded-infiltration submodel were derived from mass balance of water and ammoniacal N. The following simplifications were introduced in this submodel: (i) swine effluent was surface applied instantaneously in a flood irrigation event; (ii) distribution of ammoniacal N is uniform in the ponding layer.

Another submodel for droplet volatilization was developed to estimate ammoniacal N concentration of a droplet when it hits the ground. Droplet ammonium concentration at the soil surface is needed to specify the upper boundary condition of the transport-and-transformation model during a sprinkler-irrigation event. The droplet-volatilization submodel also evaluates the loss of ammoniacal N from a droplet during its exposure time in the air. Equations of the droplet volatilization submodel were derived from mass and energy balance in a droplet. Distributions of ammoniacal N and liquid temperature inside a droplet were assumed uniform in the derivation.

### Development of the Transport-and-Transformation Model

#### Mass Balance of Ammoniacal Nitrogen in Soils

Transport of ammoniacal N in a soil system is a multiphase, multispecies process. There are ammonium ions ( $\text{NH}_4^+(\text{aq})$ ) and dissolved ammonia ( $\text{NH}_3(\text{aq})$ ) in soil solution, gaseous ammonia ( $\text{NH}_3(\text{g})$ ) in soil air, adsorbed  $\text{NH}_4^+(\text{ad})$  and  $\text{NH}_3(\text{ad})$  at the solid-liquid interface, and adsorbed  $\text{NH}_3(\text{ad})$  at the solid-air interface. The total concentration of ammoniacal N in a soil system is the sum of the concentrations of all the component species in the three phases of the soil system

$$C_t = \left[ \begin{array}{l} \rho_b S_{\text{NH}_4^+(\text{aq})} + \theta C_{\text{NH}_4^+(\text{aq})} \\ + \rho_b S_{\text{NH}_3(\text{aq})} + \theta C_{\text{NH}_3(\text{aq})} \\ + \rho_b S_{\text{NH}_3(\text{g})} + (\theta_s - \theta) C_{\text{NH}_3(\text{g})} \end{array} \right] \quad [1]$$

where  $C_t$  is the total concentration of ammoniacal N in a soil system, which is defined as the amount of ammoniacal N in unit bulk volume of soil ( $\text{kg m}^{-3}$  bulk soil);  $S_{\text{NH}_4^+(\text{aq})}$  is the concentration of ammoniacal N in the form of adsorbed ammonium ion at the solid-liquid interface ( $\text{kg kg}^{-1}$  dry soil);  $S_{\text{NH}_3(\text{aq})}$  is the concentration of ammoniacal N in the form of adsorbed ammonia at the solid-liquid interface ( $\text{kg kg}^{-1}$  dry soil);  $S_{\text{NH}_3(\text{g})}$  is the

concentration of ammoniacal N in the form of adsorbed ammonia at the solid–air interface ( $\text{kg kg}^{-1}$  dry soil);  $C_{\text{NH}_4^+(\text{aq})}$  is the concentration of ammoniacal N in the form of ammonium ion in soil solution ( $\text{kg m}^{-3}$  solution);  $C_{\text{NH}_3(\text{aq})}$  is the concentration of ammoniacal N in the form of dissolved ammonia in soil solution ( $\text{kg m}^{-3}$  solution);  $C_{\text{NH}_3(\text{g})}$  is the concentration of ammoniacal N in the form of gaseous ammonia in soil air ( $\text{kg m}^{-3}$  soil air);  $\rho_b$  is the bulk density of the soil ( $\text{kg m}^{-3}$ );  $\theta_s$  is the porosity of the soil ( $\text{m}^3 \text{m}^{-3}$ ); and  $\theta$  is the water content of the soil ( $\text{m}^3 \text{m}^{-3}$ ).

The total flux of ammoniacal N crossing a horizontal plane is the sum of the dispersive and convective fluxes for aqueous ammonium ion and ammonia in soil solution and the diffusive flux for gaseous ammonia in soil air. Mathematically the total flux can be expressed as

$$J_t = \begin{bmatrix} -D_{\text{NH}_4^+(\text{aq})} \frac{\partial C_{\text{NH}_4^+(\text{aq})}}{\partial z} + q C_{\text{NH}_4^+(\text{aq})} \\ -D_{\text{NH}_3(\text{aq})} \frac{\partial C_{\text{NH}_3(\text{aq})}}{\partial z} + q C_{\text{NH}_3(\text{aq})} \\ -D_{\text{NH}_3(\text{g})} \frac{\partial C_{\text{NH}_3(\text{g})}}{\partial z} \end{bmatrix} \quad [2]$$

where  $J_t$  the total flux of ammoniacal N crossing a horizontal plane ( $\text{kg m}^{-2} \text{s}^{-1}$ );  $D_{\text{NH}_4^+(\text{aq})}$  is the dispersion coefficient of ammonium ion in soil solution ( $\text{m}^2 \text{s}^{-1}$ );  $D_{\text{NH}_3(\text{aq})}$  is the dispersion coefficient of dissolved ammonia in soil solution ( $\text{m}^2 \text{s}^{-1}$ );  $D_{\text{NH}_3(\text{g})}$  is the diffusion coefficient of gaseous ammonia in soil air ( $\text{m}^2 \text{s}^{-1}$ );  $q$  is the flux density of soil solution ( $\text{m s}^{-1}$ );  $t$  is time (s); and  $z$  is the vertical coordinate starting from the soil surface and positive downward (m).

Within a relatively short period (such as a week) during and after a swine effluent-irrigation event, the contribution of ammoniacal N from mineralization of soil organic matter and the loss of ammoniacal N because of immobilization (such as plant uptake) and nitrification are expected to be negligible compared with ammonia volatilization from soil surface. Neglecting the effect of mineralization, immobilization, and nitrification, the mass balance of ammoniacal N in a soil system can be expressed as

$$\frac{\partial C_t}{\partial t} = -\frac{\partial J_t}{\partial z} \quad [3]$$

### Transformation of Ammoniacal Nitrogen in Soils

Ammoniacal N in swine effluent exists mainly in two species:  $\text{NH}_4^+(\text{aq})$  and  $\text{NH}_3(\text{aq})$ . Upon entering a soil system, the two component species are distributed into the three phases of the soil system through adsorption–desorption reactions at the solid–liquid and solid–air interfaces, and the transformation of  $\text{NH}_3(\text{aq})$  into  $\text{NH}_3(\text{g})$  at the liquid–air interface. Assuming a linear equilibrium isotherm for the adsorption–desorption reactions, concentrations of the adsorbed species are related to those of their corresponding reactants by the following system of equations:

$$\begin{aligned} S_{\text{NH}_4^+(\text{aq})} &= K_{\text{NH}_4^+(\text{aq})} C_{\text{NH}_4^+(\text{aq})} \\ S_{\text{NH}_3(\text{aq})} &= K_{\text{NH}_3(\text{aq})} C_{\text{NH}_3(\text{aq})} \\ S_{\text{NH}_3(\text{g})} &= K_{\text{NH}_3(\text{g})} C_{\text{NH}_3(\text{g})} \end{aligned} \quad [4]$$

where  $K_{\text{NH}_4^+(\text{aq})}$  is the partition coefficient for liquid-phase ammonium ion ( $\text{m}^3 \text{kg}^{-1}$ ),  $K_{\text{NH}_3(\text{aq})}$  is the partition coefficient for liquid-phase ammonia ( $\text{m}^3 \text{kg}^{-1}$ ), and  $K_{\text{NH}_3(\text{g})}$  is the partition coefficient for gas-phase ammonia ( $\text{m}^3 \text{kg}^{-1}$ ). The concentrations of ammonium ion and dissolved ammonia in soil solution are related to each other by

$$K_a = \frac{C_{\text{NH}_3(\text{aq})} C_{\text{H}_3\text{O}^+(\text{aq})}}{C_{\text{NH}_4^+(\text{aq})}} \quad [5]$$

where  $K_a$  is an equilibrium constant for the following Bronstead acid-base reaction in soil solution:



$C_{\text{H}_3\text{O}^+(\text{aq})}$  is the molar concentration of hydronium ion in soil solution ( $\text{mol L}^{-1}$ ) and is related to soil pH by

$$C_{\text{H}_3\text{O}^+(\text{aq})} = 10^{-\text{pH}} \quad [7]$$

Assuming instantaneous equilibrium between gas-phase and liquid-phase ammonia, we have

$$C_{\text{NH}_3(\text{g})} = K_H C_{\text{NH}_3(\text{aq})} \quad [8]$$

where  $K_H$  is Henry's constant for the dissolution of ammonia in soil solution.

Equations [4], [5], and [8] reveal that under equilibrium conditions the concentrations of all the component species of ammoniacal N in a soil system are related to each other. Given the concentration of any of the component species, the concentrations of all other component species and the total concentration of ammoniacal N in the soils system can be evaluated from the known concentration.

### Governing Equation and Parameter Specification

Substituting the total concentration and total flux of ammoniacal N in Eq. [1] and [2] into Eq. [3] of mass balance gives

$$\begin{aligned} \frac{\partial}{\partial t} \left[ \begin{aligned} &\rho_b S_{\text{NH}_4^+(\text{aq})} + \theta C_{\text{NH}_4^+(\text{aq})} \\ &+ \rho_b S_{\text{NH}_3(\text{aq})} + \theta C_{\text{NH}_3(\text{aq})} \\ &+ \rho_b S_{\text{NH}_3(\text{g})} + (\theta_s - \theta) C_{\text{NH}_3(\text{g})} \end{aligned} \right] = \\ \frac{\partial}{\partial z} \left[ \begin{aligned} &D_{\text{NH}_4^+(\text{aq})} \frac{\partial C_{\text{NH}_4^+(\text{aq})}}{\partial z} - q C_{\text{NH}_4^+(\text{aq})} \\ &+ D_{\text{NH}_3(\text{aq})} \frac{\partial C_{\text{NH}_3(\text{aq})}}{\partial z} - q C_{\text{NH}_3(\text{aq})} \\ &+ D_{\text{NH}_3(\text{g})} \frac{\partial C_{\text{NH}_3(\text{g})}}{\partial z} \end{aligned} \right] \end{aligned} \quad [9]$$

Selecting the concentration of ammonium ion in solution as a dependent variable, plugging in the relationships between concentrations of the component species in the Eq. [4], [5], and [8] into Eq. [9], and rearranging



yield the following governing equation for ammoniacal N transport in a soil profile

$$\frac{\partial}{\partial t} \left[ \left( \rho_b K_d + \left( 1 + \frac{K_a}{10^{-\text{pH}}} \right) \theta + (\theta_s - \theta) \frac{K_a K_H}{10^{-\text{pH}}} \right) C_{\text{NH}_4^+(\text{aq})} \right] = \frac{\partial}{\partial z} \left[ D \frac{\partial C_{\text{NH}_4^+(\text{aq})}}{\partial z} - \left( 1 + \frac{K_a}{10^{-\text{pH}}} \right) q C_{\text{NH}_4^+(\text{aq})} \right] \quad [10]$$

where

$$K_d = K_{\text{NH}_4^+(\text{aq})} + K_{\text{NH}_3(\text{aq})} \frac{K_a}{10^{-\text{pH}}} + K_{\text{NH}_3(\text{g})} \frac{K_a K_H}{10^{-\text{pH}}} \quad [11]$$

and

$$D = D_{\text{NH}_4^+(\text{aq})} + D_{\text{NH}_3(\text{aq})} \frac{K_a}{10^{-\text{pH}}} + D_{\text{NH}_3(\text{g})} \frac{K_a K_H}{10^{-\text{pH}}} \quad [12]$$

The dispersion coefficients,  $D_{\text{NH}_4^+(\text{aq})}$ , and  $D_{\text{NH}_3(\text{aq})}$ , and diffusion coefficient,  $D_{\text{NH}_3(\text{g})}$  in a soil system are related to the corresponding coefficients in water and air by (Marshall and Holmes, 1988; Moldrup et al., 1997; Olesen et al., 1999)

$$\begin{aligned} D_{\text{NH}_4^+(\text{aq})} &= \alpha_L |q| + \theta \tau_w(\theta) D_{\text{NH}_4^+, \text{water}} \\ D_{\text{NH}_3(\text{aq})} &= \alpha_L |q| + \theta \tau_w(\theta) D_{\text{NH}_3, \text{water}} \\ D_{\text{NH}_3(\text{g})} &= (\theta_s - \theta) \tau_a(\theta) D_{\text{NH}_3, \text{air}} \end{aligned} \quad [13]$$

where  $\alpha_L$  is the dispersivity of the soil medium ( $m$ ),  $D_{\text{NH}_4^+, \text{water}}$  is the diffusion coefficient of ammonium ion in water ( $\text{m}^2 \text{s}^{-1}$ ),  $D_{\text{NH}_3, \text{water}}$  is the diffusion coefficient of dissolved ammonia in water ( $\text{m}^2 \text{s}^{-1}$ ),  $\tau_w(\theta)$  is the impedance factor of water flow path in the soil medium at a water content  $\theta$ ,  $D_{\text{NH}_3, \text{air}}$  is the diffusion coefficient of ammonia in free air ( $\text{m}^2 \text{s}^{-1}$ ),  $\tau_a(\theta)$  is the impedance factor of the air flow path in the soil medium at a water content  $\theta$ . The dependence of the impedance factors on soil-water content can be expressed as (Moldrup et al., 1997; Olesen et al., 1999)

$$\begin{aligned} \tau_w(\theta) &= \begin{cases} 0.45 \frac{\theta - 0.022b}{\theta_s - 0.022b}, & \theta > 0.022b \\ 0, & \theta \leq 0.022b \end{cases} \\ \tau_a(\theta) &= 0.45 \left( \frac{\theta_s - \theta}{\theta_s} \right)^{1+3/b} \end{aligned} \quad [14]$$

where 0.022b equals the threshold soil water content at which solute diffusion ceases because of disconnection of the continuous water films,  $b$  is a pore-size distribution parameter which is estimated from the percentages of clay and fine sand particles using the equation (Moldrup et al., 1997; Williams et al., 1992)

$$b = \frac{1}{0.303 - 0.093 \ln(\rho_b) - 0.0565 \ln(f_{\text{clay}}) + 0.00003 f_{\text{FS}}^2} \quad [15]$$

where  $f_{\text{clay}}$  and  $f_{\text{FS}}$  are the mass percentages of clay (<0.002 mm in diameter) and fine sand (0.02–0.2 mm in diameter) particles, respectively.

## Temperature Dependence of Transformation and Transport Parameters

The equilibrium constant  $K_a$ , Henry's constant  $K_H$ , and diffusion coefficients  $D_{\text{NH}_4^+, \text{water}}$ ,  $D_{\text{NH}_3, \text{water}}$ , and  $D_{\text{NH}_3, \text{air}}$  vary with temperature. The following empirical formulas were used to describe the dependence of these parameters on temperature (Beutier and Renon, 1978; Gernermont and Cellier, 1997):

$$\begin{aligned} \ln(K_a) &= -177.95 - \frac{1843}{T} + 31.434 \ln(T) - 0.0545T \\ \ln(RTK_H) &= 158.17 - \frac{8621}{T} - 25.677 \ln(T) + 0.0354T \\ D_{\text{NH}_4^+, \text{water}} &= D_{\text{NH}_4^+, \text{water}}^{\text{Ref}} 1.03^{(T-T_{\text{Ref}})} \\ D_{\text{NH}_3, \text{water}} &= D_{\text{NH}_3, \text{water}}^{\text{Ref}} 1.03^{(T-T_{\text{Ref}})} \\ D_{\text{NH}_3, \text{air}} &= D_{\text{NH}_3, \text{air}}^{\text{Ref}} 1.03^{(T-T_{\text{Ref}})} \end{aligned} \quad [16]$$

where  $T$  (K) is the temperature of the fluids in which the acid-base reaction, liquid-gas transformation, and aqueous and gaseous diffusion occur, and  $R$  is the universal gas constant ( $0.008315 \text{ kJ mol}^{-1} \text{ K}^{-1}$ ). In this model we assume that the temperature of the soil solution is the same as that of the bulk soil. During ponding infiltration, we assume that the temperature of the ponding layer is the same as the temperature of the ambient air.  $D_{\text{NH}_4^+, \text{water}}^{\text{Ref}}$ ,  $D_{\text{NH}_3, \text{water}}^{\text{Ref}}$ , and  $D_{\text{NH}_3, \text{air}}^{\text{Ref}}$  ( $\text{m}^2 \text{s}^{-1}$ ) are the diffusion coefficients at a reference temperature,  $T_{\text{Ref}}$  (K). At 25°C, the diffusion coefficients of aqueous ammonium ion and gaseous ammonia were taken as  $1.96 \times 10^{-9} \text{ m}^2 \text{s}^{-1}$  (Kemper, 1986) and  $2.8 \times 10^{-5} \text{ m}^2 \text{s}^{-1}$  (Incropera and DeWitt, 1990), respectively. The diffusion coefficient of dissolved ammonia was also taken as  $1.96 \times 10^{-9} \text{ m}^2 \text{s}^{-1}$ .

## Boundary Conditions for the Transport of Ammoniacal Nitrogen in a Soil Profile

**Upper Boundary.** Transport and transformation of ammoniacal N at the upper boundary of a soil profile under swine-effluent irrigation is dependent on the way the effluent is delivered to soil surface. During a flood-irrigation event, the total flux of ammoniacal N into a soil profile equals the flux entering the soil profile with the infiltrating water. That is

$$J_{I|z=0} = \left( 1 + \frac{K_a^0}{10^{-\text{pH}_0}} \right) q_0 C_{\text{NH}_4^+(\text{aq})}^0 \quad [17]$$

where  $J_{I|z=0}$  is the total flux of ammoniacal N into a soil profile ( $\text{m s}^{-1} \text{ g L}^{-1}$ );  $K_a^0$  is the equilibrium constant of the  $\text{NH}_4^+(\text{aq}) \leftrightarrow \text{NH}_3(\text{aq})$  reaction in the ponding layer of the irrigated effluent;  $\text{pH}_0$  is the pH value of the swine effluent in the ponding layer;  $C_{\text{NH}_4^+(\text{aq})}^0$  ( $\text{g L}^{-1}$ ) is the average concentration of ammoniacal N in the form of ammonium ion in the ponding layer;  $q_0$  ( $\text{m d}^{-1}$ ) is the infiltration flux of swine effluent into the soil profile from the ponding layer.  $C_{\text{NH}_4^+(\text{aq})}^0$  is evaluated in the submodule for flood irrigation.  $q_0$  is evaluated in the submodule for water flow.

During a sprinkler-irrigation event, the net flux of

ammoniacal N into a soil profile equals the flux entering the soil profile with the infiltrating water minus the volatilization flux from soil surface. That is

$$J_t|_{z=0} = \left(1 + \frac{K_a^{\text{drop}}}{10^{-\text{pH}_{\text{drop}}}}\right) i_r C_{\text{NH}_4^+}^{\text{drop}}(\text{aq}) - \left(\frac{\theta_0}{\theta_s}\right) h_m [C_{\text{NH}_3(\text{g})}|_{z=0} - C_{\text{NH}_3(\text{g})}^{\text{air}}] \quad [18]$$

where  $K_a^{\text{drop}}$  is the equilibrium constant of the  $\text{NH}_4^+(\text{aq}) \leftrightarrow \text{NH}_3(\text{aq})$  reaction in a droplet of a sprinkler-irrigation event;  $\text{pH}_{\text{drop}}$  is the pH value of the swine effluent in the droplet;  $i_r$  is the effective intensity of the sprinkler irrigation event ( $\text{m s}^{-1}$ );  $C_{\text{NH}_4^+}^{\text{drop}}(\text{aq})$  ( $\text{g L}^{-1}$ ) is the average concentration of ammoniacal N in the form of ammonium ion in the droplet;  $C_{\text{NH}_3(\text{g})}|_{z=0}$  is the concentration of ammoniacal N in the form of gaseous ammonia at the soil surface ( $\text{g L}^{-1}$ );  $C_{\text{NH}_3(\text{g})}^{\text{air}}$  is the background concentration of ammoniacal N in the form of ammonia in the air ( $\text{g L}^{-1}$ );  $\theta_0$  is soil water content at the surface, and  $h_m$  ( $\text{m s}^{-1}$ ) is the average mass transfer coefficient for ammonia transport across an ammonia concentration boundary layer at the soil surface of an irrigated strip. Because of ammonia volatilization from droplet surfaces, the ammoniacal N concentration of a droplet at the time it hits the ground may be different from the concentration of the source effluent. The ammoniacal N concentration in Eq. [18] is the average concentration of all the droplets of a sprinkler system at the time the droplets hit the ground. The average droplet concentration,  $C_{\text{NH}_4^+}^{\text{drop}}(\text{aq})$ , is estimated in a droplet-volatilization submodule (Wu et al., 2002). The average mass transfer coefficient,  $h_m$ , is estimated using the following empirical equation established for mass transfer across a turbulent-flow-dominated concentration boundary layer on a hydraulically smooth flat plate in a parallel flow of a binary fluid mixture (Genermont and Cellier, 1997; Incropera and DeWitt, 1990; Schlichting, 1968)

$$h_m = 0.037 \frac{D_{\text{NH}_3, \text{air}}}{L} \left(\frac{u_\infty L}{\nu}\right)^{4/5} \left(\frac{\nu}{D_{\text{NH}_3, \text{air}}}\right)^{1/3} \quad [19]$$

where  $L$  is the width of the irrigated strip in the wind direction ( $\text{m}$ );  $u_\infty$  is the wind speed across the irrigated strip ( $\text{m s}^{-1}$ );  $\nu$  is the kinematic viscosity of the air ( $\text{m}^2 \text{s}^{-1}$ ). The kinematic viscosity  $\nu$  is dependent on temperature and values of  $\nu$  at different air temperatures were obtained through linear interpolation using the base points given by Incropera and DeWitt (1990).

The upper boundary condition for ammoniacal N transport in a soil profile after an irrigation event can be expressed as

$$J_t|_{z=0} = -\left(\frac{\theta_0}{\theta_s}\right) h_m [C_{\text{NH}_3(\text{g})}|_{z=0} - C_{\text{NH}_3(\text{g})}^{\text{air}}] \quad [20]$$

The gas-phase ammonia concentration at the soil surface is dependent on the concentration of ammonium ion in soil solution

$$C_{\text{NH}_4^+}(\text{aq})|_{z=0} = \left[\frac{K_a K_H}{10^{-\text{pH}}} C_{\text{NH}_4^+}(\text{aq})\right]_{z=0} \quad [21]$$

**Lower Boundary.** The lower boundary for ammoniacal N transport in the soil profile can be set at a depth deep enough that the ammoniacal N from the manure application never reaches that depth, therefore

$$C_{\text{NH}_3(\text{g})}|_{z=Z_N} = 0 \quad [22]$$

where  $Z_N$  is the depth set as the lower boundary for the transport of ammoniacal N ( $\text{m}$ ).

### Development of the Ponded-Infiltration Submodel

Assuming that the concentration of ammoniacal N in the infiltration pond is uniformly distributed, the mass balance of ammoniacal N in an infiltrating pond surrounded by an elevated border can be expressed as

$$\frac{d}{dt}[h^0(t)(C_{\text{NH}_4^+}^0(\text{aq}) + C_{\text{NH}_3(\text{aq})}^0)] = -h_m(C_{\text{NH}_3(\text{g})}^0 - C_{\text{NH}_3(\text{g})}^{\text{air}}) - q_0(C_{\text{NH}_4^+}^0(\text{aq}) + C_{\text{NH}_3(\text{aq})}^0) \quad [23]$$

where  $C_{\text{NH}_3(\text{aq})}^0$  ( $\text{g L}^{-1}$ ) is the concentration of ammoniacal N in the form of aqueous ammonia in the infiltration pond;  $C_{\text{NH}_3(\text{g})}^0$  ( $\text{g L}^{-1}$ ) is the concentration of ammoniacal N in the form of gaseous ammonia at the liquid-air interface of the infiltration pond;  $h^0(t)$  is the thickness of the ponding layer ( $\text{m}$ );  $C_{\text{NH}_4^+}^0(\text{aq})$ ,  $C_{\text{NH}_3(\text{g})}^{\text{air}}$ ,  $q_0$ , and  $h_m$  are defined in the Eq. [17] and [18].

Applying Eq. [5] to [8] to the transformation of ammoniacal N in the infiltration pond, we obtain

$$K_a^0 = \frac{C_{\text{NH}_3(\text{aq})}^0 C_{\text{H}_3\text{O}^+(\text{aq})}^0}{C_{\text{NH}_4^+}^0(\text{aq})} \\ C_{\text{H}_3\text{O}^+(\text{aq})}^0 = 10^{-\text{pH}_0} \\ C_{\text{NH}_3(\text{g})}^0 = K_H^0 C_{\text{NH}_3(\text{aq})}^0 \quad [24]$$

where  $C_{\text{H}_3\text{O}^+(\text{aq})}^0$  is the molar concentration of hydronium ion in the infiltrating pond ( $\text{mol L}^{-1}$ );  $K_H^0$  is the Henry's constant for the dissolution of ammonia in the infiltrating pond;  $K_a^0$  and  $\text{pH}_0$  are defined in Eq. [17].

Expanding Eq. [23], substituting Eq. [24] into the expanded equation, and taking into account the fact that  $\frac{dh^0(t)}{dt} = -q_0$  yields

$$h^0(t) \frac{d}{dt} \left[ \left(1 + \frac{K_a^0}{10^{-\text{pH}_0}}\right) C_{\text{NH}_4^+}^0(\text{aq}) \right] = -h_m \left( \frac{K_a^0 K_H^0}{10^{-\text{pH}_0}} C_{\text{NH}_4^+}^0(\text{aq}) - C_{\text{NH}_3(\text{g})}^{\text{air}} \right) \quad [25]$$

Introducing  $\alpha(t) = 1 + \frac{K_a^0}{10^{-\text{pH}_0}}$ ,  $\beta(t) = \frac{K_a^0 K_H^0}{\alpha(t) 10^{-\text{pH}_0}}$ , and  $y = \alpha(t) C_{\text{NH}_4^+}^0(\text{aq})$ , and rearranging Eq. [25], we obtain



$$\frac{dy}{dt} + \frac{h_m \beta(t)}{h^0(t)} y = \frac{h_m}{h^0(t)} C_{\text{NH}_3(\text{g})}^{\text{air}} \quad [26]$$

Solving Eq. [26] using the variation-of-parameter method (Loomis, 1982) and replacing  $y$  with  $\alpha(t)C_{\text{NH}_4^+(\text{aq})}^0$  yields

$$C_{\text{NH}_4^+(\text{aq})}^0 = \frac{\exp\left(-\int_0^t \frac{h_m \beta(t)}{h^0(t)} dt\right)}{\alpha(t)} \left[ \alpha(0)C_{\text{NH}_4^+(\text{aq})}^0(0) + \int_0^t \exp\left(\int_0^t \frac{h_m \beta(t)}{h^0(t)} dt\right) \frac{h_m}{h^0(t)} C_{\text{NH}_3(\text{g})}^{\text{air}} dt \right] \quad [27]$$

where  $\alpha(0)$  is the value of  $\alpha$  at time zero;  $C_{\text{NH}_4^+(\text{aq})}^0(0)$  is the initial concentration of ammoniacal N in the form of ammonium ion in the irrigated-swine effluent ( $\text{g L}^{-1}$ ). Variations of  $\alpha$  and  $\beta$  are caused by the temperature dependence of the equilibrium constant  $K_a^0$  and the Henry's constant  $K_H^0$ , and the fluctuation of air temperature with time.

### Coupling the Component Modules

Distributions of soil-water content and soil temperature in a profile are needed to evaluate the coefficients in the governing equation of ammoniacal N transport. Soil-water contents and soil temperatures in a profile are obtained by solving the water flow and heat flow equations. Since the volumetric heat capacity and thermal conductivity of a soil system are dependent on soil-water content (Hillel, 1998; Scott, 2000; Wu and Nofziger, 1999), the water flow equation must be solved before the heat flow equation. Because of the nonlinearity in the governing equation of water flow and the complexity in the expressions of the coefficients in all the governing equations and boundary conditions, numerical methods are employed to solve the problems. Temporal variations of the concentrations of ammoniacal N in a soil profile and the amount and rate of ammonia volatilization from soil surface are obtained by solving the initial-boundary problems of N transport, water flow, and heat flow in a stepwise manner. At each time step, the model evaluates the concentrations of ammoniacal N, soil-water potentials, and soil temperatures in a profile at the end of the time interval from those at the beginning of the interval. The water flow problem was solved first at a time step to determine water contents and Darcy velocities in the profile. Then the heat flow problem was solved for soil temperatures in the profile using the volumetric heat capacity and thermal conductivity calculated from water contents obtained in the solution of the water-flow problem (Farouki, 1986; Hillel, 1998; Wu and Nofziger, 1999). Measured data of hourly air temperature were used as the surface-soil temperature at the upper boundary of the heat-flow problem. The lower boundary was set at a location deep enough that soil temperature at such a depth is not significantly affected by temperature fluctuations at the soil surface. Since the lower boundary of the heat-flow problem was at a much deeper location than that of the water-flow and transport problems, mesh points used

to solve the heat-flow problem are different from those used to solve the water-flow and transport problems. Linear interpolation was employed to evaluate soil temperatures at the mesh points of the water-flow and transport problems. Water contents at the mesh points of the heat-flow problem were also evaluated by interpolation. At locations below the lower boundary of the water-flow and transport problems, water contents at the mesh points of the heat-flow problem were set at the water content of the mesh point at the lower boundary of the water-flow and transport problem. Finally the N transport problem was solved for concentrations of ammoniacal N in the soil profile using the storage and transport parameters calculated from the water contents, Darcy velocities, and soil temperatures obtained in the solutions of water-flow and heat-flow problems.

During the infiltration phase of an irrigation event, a submodel is invoked at each time step to evaluate the concentration of ammoniacal N entering the soil profile. The submodel invoked is dependent on the irrigation method used. In the case of flood irrigation, Eq. [27] is used to calculate concentration of ammoniacal N entering the soil profile. For a sprinkler-irrigation event, the droplet volatilization model (Wu et al., 2002) is invoked to evaluate the average droplet concentration of ammoniacal N at the soil surface. The droplet volatilization model also calculates the amount of droplet volatilization of ammoniacal N from the sprinkler system.

### Evaluating Rate and Amount of Ammonia Volatilization

A major objective of this model is to estimate the rate and amount of ammonia volatilization from surface-applied swine effluent. Like the specification of the upper boundary condition for the transport of ammoniacal N in a soil profile, the method for evaluating the rate and amount of ammonia volatilization is dependent on the irrigation method used to deliver swine effluent to a soil surface. During the infiltration phase of a flood-irrigation event, ammonia volatilization occurs at the liquid-air interface of the ponding layer instead of the soil surface. The volatilization rate during that time was calculated using the equation

$$J_{\text{vola}}(t) = h_m \left( \frac{K_a^0 K_H^0}{10^{-\text{pH}_0}} C_{\text{NH}_4^+(\text{aq})}^0 - C_{\text{NH}_3(\text{g})}^{\text{air}} \right) \quad [28]$$

where  $J_{\text{vola}}(t)$  is the vertical flux of ammoniacal N at time  $t$  ( $\text{kg ha}^{-1} \text{s}^{-1}$ ).

During a sprinkler-irrigation event, ammonia volatilization loss includes droplet volatilization loss, wind drift loss, and volatilization loss from soil surface. Losses from wind drift and droplet volatilization may be estimated using the efficiency-coefficient method developed by irrigation engineers for estimating water losses from wind drift and droplet evaporation (Wu et al., 2002). The soil-surface-volatilization rate during a sprinkler-irrigation event was calculated using the following equation

$$J_{\text{vola}}(t) = \left( \frac{\theta_0}{\theta_s} \right) h_m \left[ \left( \frac{K_a K_H}{10^{-\text{pH}}} C_{\text{NH}_4^+(\text{aq})} \right) \Big|_{z=0} - C_{\text{NH}_3(\text{g})}^{\text{air}} \right] \quad [29]$$

Equation [29] can also be used to evaluate soil-surface-volatilization rate during the redistribution phase after an irrigation event.

The cumulative volatilization up to time  $t$  for all the upper-boundary scenarios described above can be expressed as

$$m_{\text{NH}_3} = \int_0^t J_{\text{vola}}(t) dt \quad [30]$$

where  $m_{\text{NH}_3}$  is the cumulative amount of ammoniacal N volatilized from unit area of soil surface and the surface of the ponding layer in flood irrigation ( $\text{kg ha}^{-1}$ ).

### Model Testing

The partial differential equations for ammoniacal N transport, water flow, and heat flow in a soil profile were solved numerically using implicit finite difference schemes (Allen et al., 1988; Haverkamp et al., 1977). Explicit linearization was used to estimate the nonlinear coefficients in the water flow equation (Haverkamp et al., 1977; Nofziger et al., 1989). The numerical model was implemented in MATLAB on a PC and the computer model was tested against six sets of data from field experiments conducted in different seasons of the year (Warren, 2001; Zupancic et al., 1999).

The field experiments were conducted at the Okla-

homa State University Panhandle Research Station located in Goodwell, OK ( $36^\circ 36' 6''$  N lat.,  $101^\circ 36' 5''$  W long.) in May, July, and September of 1998, July of 1999, and March and July of 2000. The swine effluent was applied to a bare soil of a Richfield clayey loam (fine, smectitic, mesic Aridic Argiustolls) by flood irrigation. The integrated horizontal flux (IHF) method (McInnes et al., 1985; Schjoerring et al., 1992) was employed to measure the volatilization rate from a circular area of 15.24 m in diameter. Detailed information on the experiments was given by Warren (2001) and Zupancic (1999).

Figure 1 and Fig. 2 show the comparison of the measured and simulated volatilization rate and cumulative amount of ammonia volatilized. The data points of different symbols in a graph represent measured data in different replicate plots of an experiment. The solid line represents simulation results. Simulated volatilization rates in Fig. 1 are average rates over different experimental sampling periods. Input data of management-related parameters for swine-effluent irrigation events are summarized in Table 1. Input data of climate-related parameters including hourly averages of air temperature, wind speed, precipitation, and solar radiation were taken from Mesonet observations. Air temperatures and wind speeds were measured at a height of 1.5 and 2 m,

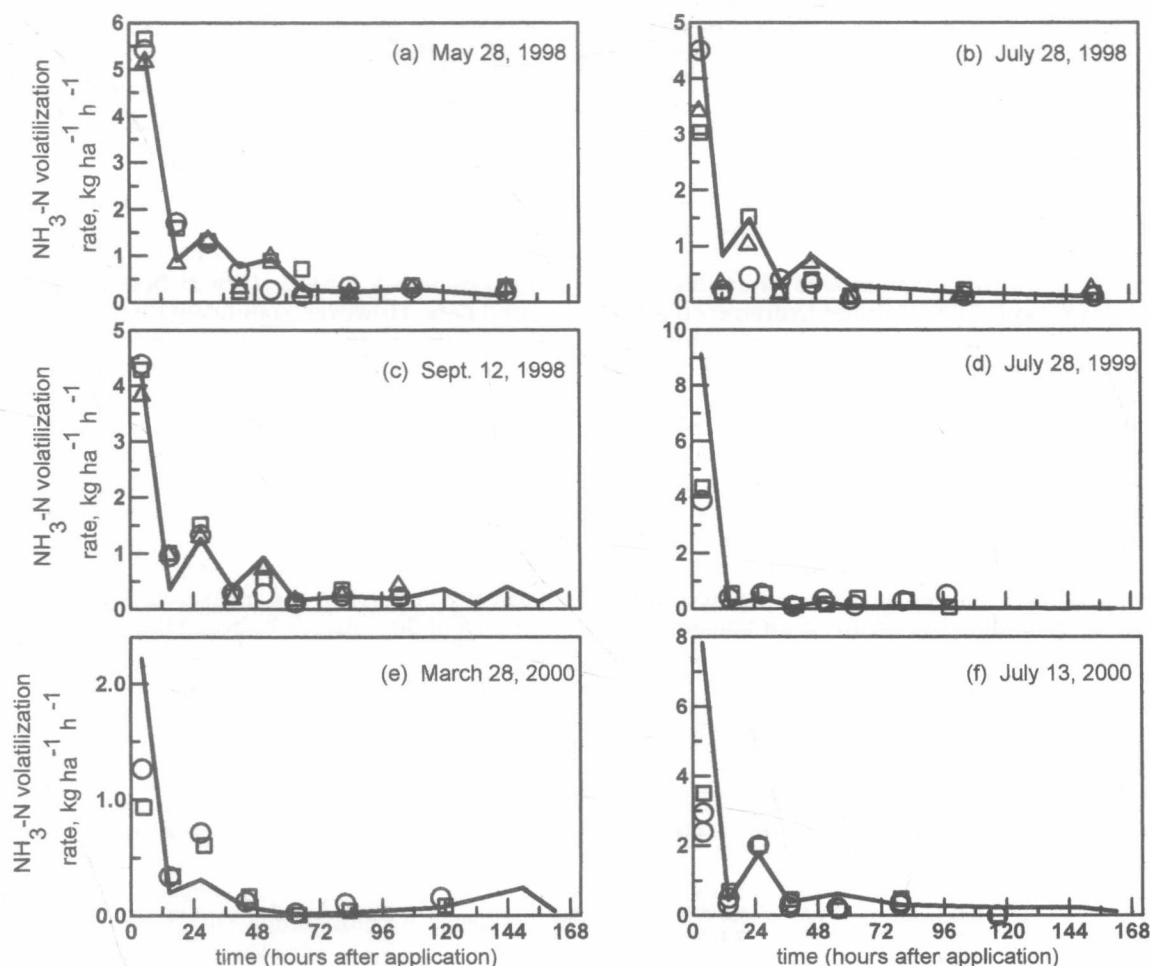


Fig. 1. Comparison of predicted average rate of ammonia volatilization loss with field data measured in different seasons. Symbols represent measured data of different replicates, and solid lines are simulation results.



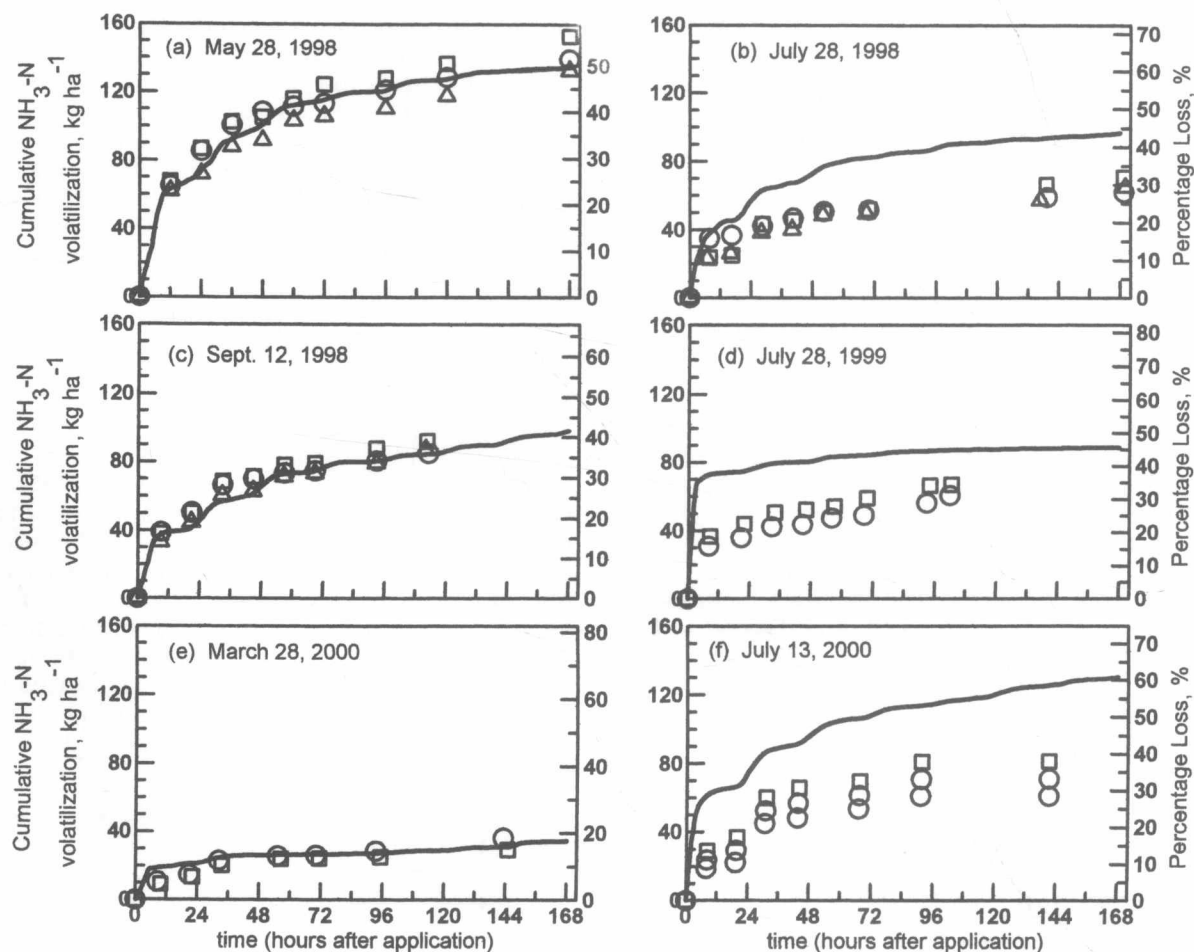


Fig. 2. Comparison of predicted cumulative ammonia volatilization loss with field data measured in different seasons. Symbols represent measured data of different replicates, and solid lines are simulation results.

respectively. The Mesonet station was within 50 m of the experimental plots. The saturated hydraulic conductivity of the soil was estimated from observed ponding duration of a swine-effluent irrigation experiment (Warren, 2001). All other soil hydraulic properties were extracted from the UNSODA unsaturated soil hydraulic database based on soil texture (Leij et al., 1996). Flow and transport parameters of the soil medium used in model testing are summarized in Table 2.

Both the experimental data and simulation results revealed large seasonal changes in percentage of volatilization loss of ammoniacal N from surface-applied swine effluent primarily because of changes in air temperature and wind speed. About 50% of ammoniacal N was lost at the end of 1 wk after a swine-effluent-irrigation event on 28 May 1998. The loss was <20% when swine effluent was applied on 28 Mar. 2000. The simulated volatiliza-

tion rate in Fig. 1(a) to 1(f) matched well with the measured data. However, significant discrepancies between the simulation results and the measured data occurred in three of the cumulative volatilization curves (see Fig. 2b, 2d, and 2f). Examining the volatilization-rate curves in Fig. 1d and 1f revealed that the discrepancies in the cumulative curves were caused mainly by the differences of the volatilization rate in the first sampling period of the experiments. Starting from the end of the first sampling period, the curves of the simulated cumulative volatilization losses in Fig. 2d and 2f are basically parallel to the measured data. In Fig. 2b, the significant discrepancy between the simulated and measured cumulative volatilization loss began at the end of the third sampling period. The simulated volatilization rate in Fig. 1b basically went through the upper limits of the measured data points. Starting from the end of

Table 1. Management-related input data from experimental records.

Starting date	NH <sub>4</sub> -N concentration	Effluent pH	Soil pH	Depth applied	Starting time	Data source
	g L <sup>-1</sup>			cm	h	
28 May 1998	0.963	7.4	8.1	2.8	1000	Zupancic, 1999
28 Jul. 1998	0.963	7.4	8.1	2.3	1400	Zupancic, 1999
12 Sept. 1998	0.963	7.4	8.1	2.4	1300	Zupancic, 1999
28 Jul. 1999	0.778	8.0	7.05	2.5	1130	Warren, 2001
28 Mar. 2000	0.782	8.25	7.62	2.5	0900	Warren, 2001
13 Jul. 2000	0.856	7.88	7.84	2.5	1230	Warren, 2001

Table 2. Flow- and transport-related input parameters.

Symbol	Description	Value	Source
$\theta_s, \text{m}^3 \text{m}^{-3}$	Saturated soil water content	0.410	Leij et al., 1996
$\theta_r, \text{m}^3 \text{m}^{-3}$	Residual soil water content	0.095	Leij et al., 1996
$\alpha_s, \text{m}^{-1}$	Empirical constant in van Genuchten's equation for hydraulic properties	1.900	Leij et al., 1996
$n_s$	Empirical constant in van Genuchten's equation for hydraulic properties	1.310	Leij et al., 1996
$K_s, \text{m s}^{-1}$	Saturated hydraulic conductivity	$9.54 \times 10^{-7}$	Derived from infiltration data
$\alpha_L, \text{m}$	Longitudinal dispersivity	0.039	Biggar and Nielsen, 1976
$K_{\text{NH}_4^+}(\text{aq}), \text{m}^3 \text{kg}^{-1}$	Adsorption-desorption coefficient of aqueous $\text{NH}_4^+$	$1.24 \times 10^{-3}$	Measured
$C_{h,s}, \text{kJ m}^{-3} \text{K}^{-1}$	Average volumetric heat capacity of soil solids	2100	Hillel, 1998
$C_{h,w}, \text{kJ m}^{-3} \text{K}^{-1}$	Volumetric heat capacity of liquid water	4200	Hillel, 1998
$\kappa_w, \text{kJ m}^{-1} \text{d}^{-1} \text{K}^{-1}$	Thermal conductivity of liquid water	51.41	van Wijk, 1963
$\kappa_a, \text{kJ m}^{-1} \text{d}^{-1} \text{K}^{-1}$	Thermal conductivity of air	2.25	van Wijk, 1963
$\kappa_s, \text{kJ m}^{-1} \text{d}^{-1} \text{K}^{-1}$	Average thermal conductivity of soil solids	$504.58-2.85f_{\text{clay}}$	Gemant, 1950
$f_{\text{clay}}, \% \text{ mass}$	Mass percentage of clay particles	32.7	Measured
$f_{\text{FS}}, \% \text{ mass}$	Mass percentage of fine sand particles	46.3	Measured

the third sampling period, the curve of the simulated cumulative volatilization loss in Fig. 2b also runs parallel to the measured data. The averages of the air temperature and wind speed for the whole week and during the first sampling period for the field experiments are summarized in Table 3.

In the IHF method, the volatilization rate was determined by integrating horizontal fluxes measured at different sampling heights. This method may underestimate the volatilization rate during the early period of an experiment when the concentration boundary layer is not fully developed. Before the top of the concentration boundary layer reached the first horizontal-flux sampler at the bottom of a sampling mast, the samplers would not catch any of the volatilized ammonia. This underestimation is expected to increase with the increase in wind speed, temperature, and the height of the first horizontal-flux sampler. The average wind speeds and air temperatures of the three experiments performed in July of 1998, 1999, and 2000 were among the highest observed (Table 3). This might explain why the measured volatilization rates in the first sampling period of these three experiments were lower than the simulated rates.

### Sensitivity Analysis

The input parameters of the mechanistic model may be divided into groups of soil-related parameters, weather-related parameters, and management-related parameters. Soil-related parameters include soil hydraulic properties, transport and reaction properties of ammoniacal N in a soil medium, and particle-size distribution of the soil medium. Weather-related parameters include wind speed, air temperature, solar radiation, and relative humidity. Management-related parameters include the amount of swine effluent applied, concentration of ammoniacal N in the effluent, effluent pH, and width in the wind direction of the field where swine effluent is applied. Figure 3 demonstrate the sensitivity of cumulative ammonia volatilization loss to soil texture, soil pH, air temperature, and wind speed. Clay-loam-textured soil, Mesonet weather data at Goodwell, OK between 28 May 1998 and 4 June 1998, and the management-related parameters from the experiment starting on 28 May 1998 were used in the simulations of sensitivity analysis if not indicated otherwise.

The difference in simulated cumulative volatilization loss at the end of 1 wk after an irrigation event between

a clay-loam textured soil and a silt-loam-textured soil is <5%. The hydraulic parameters of the clay-loam and silt-loam textured soils are shown in Table 4. A 0.2-unit decrease in soil pH from 8.1 caused an 8% decrease in simulated cumulative volatilization loss. The 0.2-unit is the expected deviation of lab-measured pH value of an individual soil sample (Dr. Hailin Zhang, personal communication, 2000). The difference in simulated volatilization loss caused by a change in soil texture from clay loam to silt loam is less than that caused by the uncertainty in lab-measured pH value of a soil sample. Changes in air temperature also resulted in considerable change in simulated cumulative volatilization loss. Raising the set of temperatures measured between 28 May 1998 and 4 June 1998 by 5°C caused a 13% increase in the simulated cumulative volatilization loss while lowering the temperatures by 5°C caused a 16% decrease in the simulated cumulative volatilization loss. The sensitivity of the simulated cumulative volatilization loss to changes in wind speed varies with the magnitude of the wind speed. Reducing the set of wind speeds measured between 28 May 1998 and 4 June 1998 by 50% caused a 13% decrease in simulated cumulative volatilization loss at the end of 1 wk while increasing the wind speeds by 50% caused a 6% increase in the simulated cumulative volatilization loss.

To aid decision-making in swine-effluent irrigation, we need to predict ammonia-volatilization loss under future weather conditions. Since future weather is unknown, historical weather data of the same season is often used for making simulations. Under such conditions, variation in weather conditions of the same season over different years largely determines the quality of the predicted results. Figure 4 shows the comparison of simulated cumulative ammonia volatilization losses from swine effluent applied to the soil surface on 28

Table 3. Weekly average air temperature and wind speed for the field experiments.

Starting date	Weekly average		First sampling period		Length
	Air temperature	Wind speed	Air temperature	Wind speed	
	°C	$\text{m s}^{-1}$	°C	$\text{m s}^{-1}$	h
28 May 1998	26.1	3.87	31.5	3.16	12.0
28 Jul. 1998	25.4	2.96	32.0	4.05	7.8
12 Sept. 1998	23.7	2.45	29.7	3.88	8.9
28 Jul. 1999	27.1	3.39	34.8	5.30	8.0
28 Mar. 2000	6.9	6.51	12.9	3.98	8.5
13 Jul. 2000	27.0	4.94	28.1	5.67	7.8

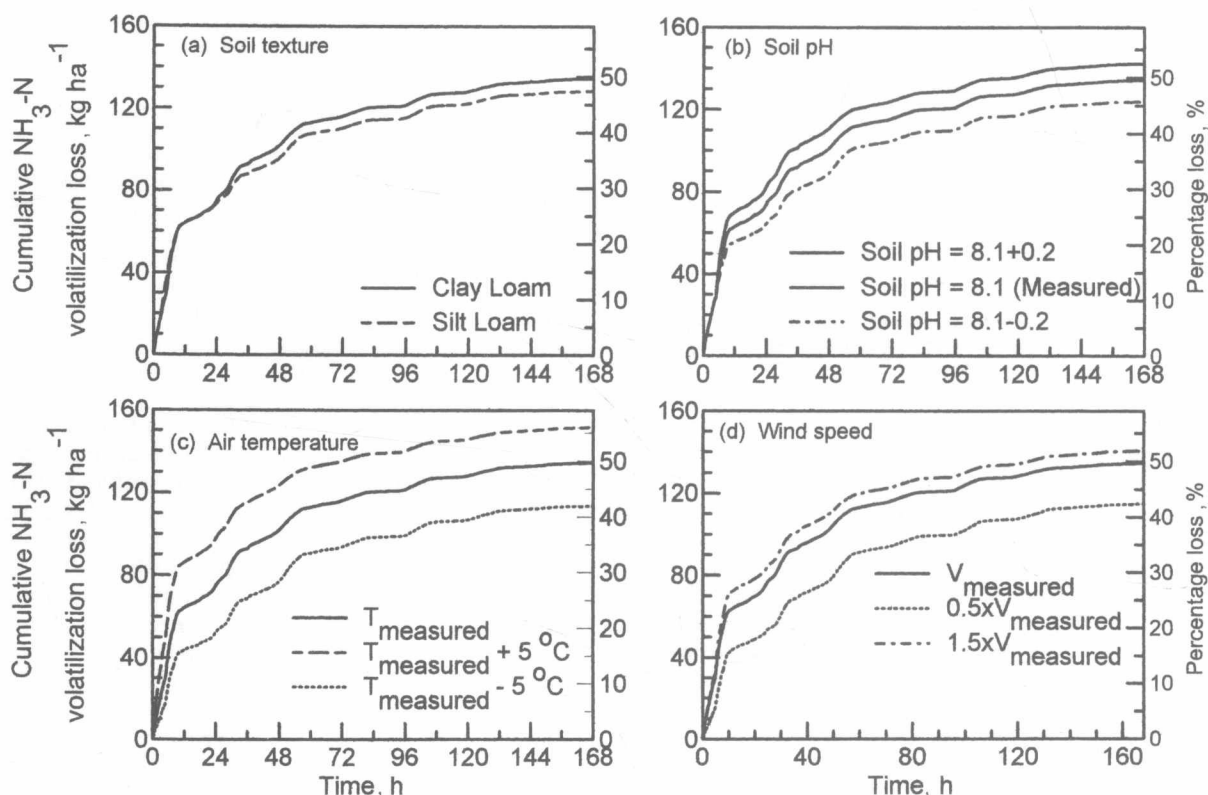


Fig. 3. Sensitivity of cumulative ammonia volatilization loss to soil texture, soil pH, air temperature, and wind speed. Time started from the beginning of simulated irrigation events.

May of 1998, 1999, and 2000 respectively. Again, hourly average Mesonet weather data were used in the simulations. Average air temperatures of the simulated period in 1998, 1999, and 2000 are 26.1, 20.8, and 25.2°C. Average wind speeds of the simulated period are 3.74, 3.85, and 5.94 m s<sup>-1</sup> for 1998, 1999, and 2000, respectively. The simulated volatilization loss in 1999 was <80% of that in 2000. The difference in volatilization loss between 1999 and 2000 was caused by a difference of 4.4°C in average air temperature, and a difference of 2.08 m s<sup>-1</sup> in average wind speed during the simulated period. Uncertainty of the simulated ammonia volatilization loss because of unknown future weather conditions at the time of application must be considered when using this model in a decision support system.

## SUMMARY AND CONCLUSIONS

A mechanistic model was developed to predict the rate and amount of ammonia volatilization from surface-applied swine effluents. The process-based model couples water flow, heat flow, and multiphase, multispecies ammoniacal N transport in a soil profile. A submo-

del was developed to predict concentrations of ammoniacal N in the infiltrating water of a flood-irrigation event and to estimate the rate and amount of ammonia volatilization from the surface of the infiltration pond. The infiltration submodel was integrated into the transport-and-transformation model to specify the upper boundary condition for the chemical transport model. The governing equations of water flow, heat flow, and the transport-and-transformation models were derived from mass and energy balances employing well-established constitutive relationships. The equations of the mechanistic model were solved numerically. The computer model was tested against the field experiments of ammonia volatilization from swine effluent applied to a field of Richfield clay loam by flood irrigation. The input parameters for the simulations were determined independently. The simulated average volatilization rate matched very well with the measured data with a few exceptions. The exceptions occurred mainly in the first sampling period of the experiments, which might be because of experimental underestimation of the vertical flux in the early stage of experiments with high wind

Table 4. Hydraulic properties of the clay-loam textured, and a silt-loam textured soils. The data were extracted from the UNSODA unsaturated soil hydraulic database (Leij et al., 1996).

Parameters	Description	Clay Loam	Silt Loam
$\theta_s$ , m <sup>3</sup> m <sup>-3</sup>	Saturated soil water content	0.410	0.450
$\theta_r$ , m <sup>3</sup> m <sup>-3</sup>	Residual soil water content	0.095	0.067
$\alpha$ , m <sup>-1</sup>	Empirical constant in van Genuchten's equation for hydraulic properties	1.900	2.000
$n$	Empirical constant in van Genuchten's equation for hydraulic properties	1.310	1.410
$K_s$ , m s <sup>-1</sup>	Saturated hydraulic conductivity	$9.54 \times 10^{-7}$	$12.5 \times 10^{-7}$



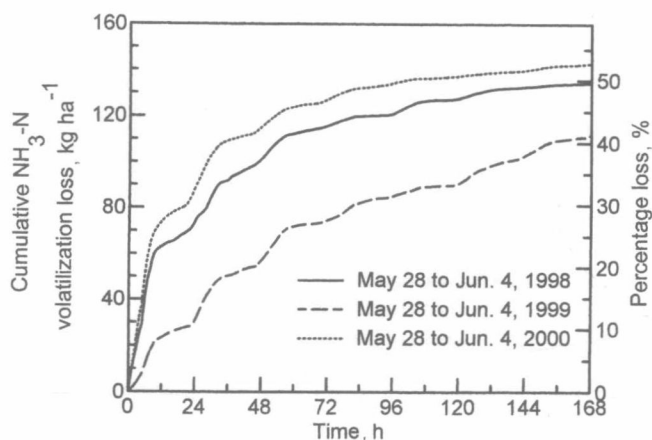


Fig. 4. Comparison of simulated cumulative ammonia volatilization loss from swine effluent applied to the soil surface on 28 May of 1998, 1999, and 2000. Hourly average Mesonet weather data were used in the simulations.

speeds. Preliminary sensitivity analysis of the model revealed significant effect of temperature fluctuation and pH variation on the simulated amount of ammonia volatilized. Variations in flow- and transport-related input parameters (except saturated hydraulic conductivity) caused relatively little change in the simulated cumulative volatilization. Further testing of the model is needed to determine if the discrepancies between simulated and measured volatilization rates arise from problems in the model or from the experimental methods employed.

## REFERENCES

- Allen, M.B., I. Herrera, and G.F. Pinder. 1988. Numerical modeling in science and engineering. John Wiley & Sons, Inc., New York.
- Asman, W.A.H., and H.A. van Jaarsveld. 1992. A variable-resolution transport model applied for  $\text{NH}_3$  in Europe. *Atmos. Environ.* 26A:445–464.
- Beutier, D., and H. Renon. 1978. Representation of  $\text{NH}_3\text{-H}_2\text{S-H}_2\text{O}$ ,  $\text{NH}_3\text{-CO}_2\text{-H}_2\text{O}$ , and  $\text{NH}_3\text{-SO}_2\text{-H}_2\text{O}$  vapor-liquid equilibria. *Ind. Eng. Chem. Process Des. Dev.* 17:220–230.
- Biggar, J.W., and D.R. Nielsen. 1976. Spatial variability of the leaching characteristics of a field soil. *Water Resour. Res.* 12:78–84.
- E.C.E.T.O.C. 1994. Ammonia emission to air in western Europe. E.C.E.T.O.C. Technical Report No. 62. E.C.E.T.O.C., Brussels, Belgium.
- Farouki, O.T. 1986. Thermal properties of soils. Series on rock and soil mechanics, vol. 11. Trans Tech Publ., Clausthal-Zellerfeld, Germany.
- Fenn, L.B., and R. Escarzagua. 1977. Ammonia volatilization from surface applications of ammonium compounds to calcareous soils: VI. Effects of initial soil water content and quantity of applied water. *Soil Sci. Soc. Am. J.* 41:358–363.
- Genermont, S., and P. Cellier. 1997. A mechanistic model for estimating ammonia volatilization from slurry applied to bare soil. *Agric. For. Meteorol.* 88:145–167.
- Haverkamp, R., M. Vauclin, J. Touma, P.J. Wierenga, and G. Vachaud. 1977. A comparison of numerical simulation models for one-dimensional infiltration. *Soil Sci. Soc. Am. J.* 41:285–294.
- Hillel, D. 1998. Environmental soil physics. Academic Press, Inc., San Diego, CA.
- Incropera, F.P., and D.P. DeWitt. 1990. Fundamentals of heat and mass transfer. John Wiley & Sons, Inc., New York.
- Ismail, K.M., F.W. Wheaton, L.W. Douglass, and W. Potts. 1991. Modeling ammonia volatilization from loamy sand soil treated with liquid urea. *Trans. ASAE* 34(3):756–763.
- Kemper, W.D. 1986. Solute diffusivity. p. 1007–1024. In A. Klute et al. (ed.) *Methods of soil analysis. Part 1.* 2nd ed. ASA and SSSA, Madison, WI.
- Khengre, S.T., and N.K. Savant. 1977. Distribution pattern of inorganic nitrogen following anhydrous ammonia injection into a Vertisol. *Soil Sci. Soc. Am. J.* 41:1139–1141.
- Kirk, G.J.D., and P.H. Nye. 1991. A model of ammonia volatilization from applied urea. VI. The effects of transient-state water evaporation. *J. Soil Sci.* 42:115–125.
- Leij, F.J., W.J. Alves, M.Th. van Genuchten, and J.R. Williams. 1996. The UNSODA unsaturated soil hydraulic database: User's manual version 1.0. National Risk Management Research Laboratory, Office of Research and Development, USEPA, Cincinnati, OH.
- Loomis, L.H. 1982. Calculus. Addison-Wesley Publishing Co., Inc., Reading, MA.
- Marshall, T.J., and J.W. Holmes. 1988. Soil physics. Cambridge University Press, New York.
- McInnes, K.J., D.E. Kissel, and E.T. Kanemasu. 1985. Estimating ammonia flux: A comparison between the integrated horizontal flux method and theoretical solutions of the diffusion profile. *Agron. J.* 77:884–889.
- Moldrup, P., T. Olesen, D.E. Rolston, and T. Yamaguchi. 1997. Modeling diffusion and reaction in soils: VII. Predicting gas and ion diffusivity in undisturbed and sieved soils. *Soil Sci.* 162:632–640.
- Nofziger, D.L., K. Rajender, S.K. Nayudu, and P. Su. 1989. CHEMFLO: One-dimensional water and chemical movement in unsaturated soils. Computer software series CSS-38. Agricultural Experiment Station, Division of agriculture, Oklahoma State University, Stillwater, OK.
- Olesen, T., P. Moldrup, and J. Gamst. 1999. Solute diffusion and adsorption in six soils along a soil texture gradient. *Soil Sci. Soc. Am. J.* 63:519–524.
- Rachhpal-Singh and P.H. Nye. 1986. A model of ammonia volatilization from applied urea. I. Development of the model. *J. Soil Sci.* 37:9–20.
- Reynolds, C.M., D.C. Wolf, and J.A. Armbruster. 1985. Factors related to urea hydrolysis in soils. *Soil Sci. Soc. Am. J.* 49:104–108.
- Schjoerring, J.K., S.G. Sommer, and M. Ferm. 1992. A simple passive sampler for measuring ammonia emission in the field. *Water Air Soil Pollut.* 62:13–24.
- Schlichting, H. 1968. Boundary-layer theory (translated by Dr. J. Keestin). McGraw-Hill, Inc., New York.
- Scott, H.D. 2000. Soil physics: Agricultural and environmental applications. Iowa State University Press, Ames, IA.
- Sutton, M.A., J.K. Schjoerring, and G.P. Wyers. 1995. Plant-atmosphere exchange of ammonia. *Philos. Trans. R. Soc. London. Ser. A* 251:261–278.
- van Wijk, W.R. (ed.) 1963. Physics of plant environment. North-Holland Publ. Co., Amsterdam.
- Warren, J.G. 2001. Ammonia volatilization from applied swine effluent in the southern great plains. M.S. thesis. Dep. of Plant and Soil Sciences, Oklahoma State University, Stillwater, OK.
- Williams, J., P. Ross, and K. Bristow. 1992. Prediction of the Campbell water retention function from texture, structure, and organic matter. p. 427–441. In M.Th. van Genuchten et al. (ed.) *Proc. Int. Workshop on indirect methods for estimating the hydraulic properties of unsaturated soils.* Riverside, CA. 11–13 Oct. 1989. University of California, Riverside, CA.
- Wu, J., and D.L. Nofziger. 1999. Incorporating temperature effects on pesticide degradation into a management model. *J. Environ. Qual.* 28:92–100.
- Wu, J., D.L. Nofziger, J.G. Warren, and J.A. Hattey. 2002. Estimating ammonia volatilization from droplets of sprinkler irrigation. *In review.*
- Zupancic, K.S. 1999. Determination of ammonia flux from swine effluent applied to calcareous soils. M.S. thesis. Dep. of Plant and Soil Sciences, Oklahoma State University, Stillwater, OK.
- Zupancic, K.S., J.A. Hattey, R. Mikkelsen, H.A. Zhang, D. Hamilton, and M. Kizer. 1999. Determination of ammonia flux from swine effluent applications in the Southern Great Plains. p. 411–414. *In Havenstein NCSU Animal Waste Management Symposium.*

# Pore-Space Dynamics in a Soil Aggregate Bed under a Static External Load

Teamrat A. Ghezzehei\* and Dani Or

## ABSTRACT

The loose and fragmented soil structure that results from tillage operations provides favorable physical conditions for plant growth. This desirable state is structurally unstable and deteriorates with time because of overburden, external stresses, and capillary forces. The objective of this study was to model these structural changes by coupling soil intrinsic rheological properties with geometry and arrangement of aggregates represented as monosized spheres. Calculations of interaggregate stresses and strains, and associated changes in density and porosity, were performed for a rhombohedral unit cell. Soil rheological properties determined by application of steady shear stress were used for calculations of strains under steady interaggregate stresses. The models developed herein correspond to the initial stage of deformation when discrete aggregates exist. At strains exceeding 0.12 the interaggregate voids are isolated and the current model no longer applies and an alternative approach is presented elsewhere. Unit cell calculations were up scaled to an aggregate-bed scale by considering a one-dimensional stack of unit cells, which allows only vertical stress transmission. The stress acting at an interaggregate contact is fully accommodated (dissipated) by viscous flow when it exceeds the yield stress (strength) of the aggregates. The stress is fully transmitted to subsequent unit cells when it is less than the yield stress. Plausibility of the models was demonstrated by illustrative examples that highlight the different features of the models. The results were in qualitative agreement with observations from the literature for deformation of either loose structure, and for highly dense cases close to maximal bulk density.

TILLAGE of agricultural soil results in a loose and fragmented structure where aggregates are separated from each other by interaggregate voids. The total volume and size distribution of these voids determine important soil physical characteristics, such as air and water conductivities, water retention, and mechanical resistance to plant root growth. This loose structure settles because of compaction by farm implements and surface tension of pore water, and consolidation by overburden (Koolen and Kuipers, 1989).

Settlement and increase in strength of agricultural soils because of various factors are often quantified using bulk empirical stress-strain relationships such as the Mohr-Coulomb curves (e.g., Horn et al., 1998; Kirby, 1994; Kirby et al., 1997; Koolen and Kuipers, 1989; Lebert et al., 1989). Often, the soil mechanical coefficients used in these constitutive relationships have no clear physical meaning (Oda and Iwashita, 1999). Moreover, bulk settlement and strength changes alone are not sufficient to describe evolution of soil hydraulic properties. Recently, we proposed alternative framework for modeling evolution of soil structure by focusing on individual soil aggregates and interaggregate pores (Ghezzehei

and Or, 2000; Ghezzehei and Or, 2001; Or, 1996). This framework considers spherical soil aggregates and interplay between soil rheology, capillary forces, and external stresses. We used stochastic formulation to upscale the single-pore dynamics to evolution of sample scale pore-size distribution (Or et al., 2000).

The objective of this study is to extend the earlier framework from the rhombic unit cell to an aggregate-bed scale by employing a simple and mechanistic up scaling scheme. This paper emphasizes static and steady external stress; extension to transient stresses such as imposed by passage of a tractor, will be presented in a subsequent work.

## THEORY

We represent a soil aggregate bed as an assembly of discrete structural units. The structural units are embodied in mathematically tractable and simple geometric constructs that retain many of the features and structural behavior of a real soil. We calculate the deformation of unit elements under the influence of steady stress using rheological properties of the soil that forms the aggregates. Subsequently, the unit element model is up scaled to an aggregate bed model by considering stress and strain propagation in a one-dimensional stack of unit elements.

### Basic Structural Unit Cell

The size, shape, and spatial arrangement of soil aggregates vary widely, and the processes of soil aggregate bed deformation nonlinearly depend on these factors. For mathematical tractability, we represent soil aggregates by spheres, and their spatial arrangements by simple packing geometries. The simplest packing systems often have the following features: (i) they are monodisperse, (ii) they are continuous, in that each sphere in the pack can be reached from any other sphere by crossing surface contacts only, and (iii) the density of the pack is uniform throughout the system. In cubic packing (Fig. 1a) each sphere is in contact with six other spheres (coordination number,  $N = 6$ ) with internal porosity ( $\phi$ ) of 47.6%. Whereas in the rhombic packing (Fig. 1b) each sphere is in contact with 12 other spheres ( $N = 12$ ) and has a porosity ( $\phi$ ) of 26.5%. For most aggregated soils the porosity of interest lies between these extremes. Two common approaches exist for building packing systems having intermediate porosity using the above unit cell configurations. In the first approach, a cubic unit cell made of eight spheres is transformed to a rhombohedral cell by sliding one of the layers, such that the displacements in the  $x$ - $y$  plane are equal. The amount of movement is given by the angle,  $\theta$ , measured between centers of spheres on the same side of the unit cell, and varies between  $90^\circ$  for cubic and  $60^\circ$  for rhombohedral (e.g., Kezdi, 1964). The formula for the porosity of the unit cell as a function of the packing angle  $\theta$  is given as

$$\phi = 1 - \frac{\pi}{6(1 - \cos\theta)\sqrt{1 + 2\cos\theta}} \quad [1]$$

In the aforementioned transformation of a unit cell, the coordination number ( $N$ ) does not vary continuously. In a second approach, the aggregate system is represented as a

T.A. Ghezzehei, Earth Science Division, Lawrence Berkeley National Laboratory, One Cyclotron Road, MS90-1116, Berkeley, CA 94720; D. Or, Dep. of Civil and Environmental Engineering, University of Connecticut, 261 Glenbrook Road, Unit 2037, Storrs, CT 06269. Received 10 Oct. 2001. \*Corresponding author (TAGhezzehei@lbl.gov).